AIAA JOURNAL
Vol. 45, No. 2, February 2007

# Sensing and Control of Combustion Instabilities in Swirl-Stabilized Combustors Using Diode-Laser Absorption

Hejie Li,* Xin Zhou,† Jay B. Jeffries,‡ and Ronald K. Hanson§
*Stanford University, Stanford, California 94305-3032*

DOI: 10.2514/1.24774

**Thermoacoustic instability and lean blowout are monitored in propane/air flames in a swirl-stabilized combustor using a novel tunable diode-laser sensor for gas temperature using wavelength-scanned laser absorption of two neighboring water vapor transitions near 1.4 $\mu$m. Although the gas composition and temperature are not uniform along the sensor line of sight, temperature oscillations and fluctuations are clearly identified in the fast Fourier transform power spectra of the time-resolved data. Detailed experiments are conducted to optimize the position of the sensor line of sight in the flame for thermoacoustic instability and lean-blowout sensing. The output of the sensor is used to suppress the thermoacoustic oscillations in a phase-delay feedback control system, and acoustic modulation of the intake air flow suppresses the temperature oscillations by more than 7 dB. The low-frequency temperature fluctuations measured by the tunable diode-laser sensor increase sharply as the flame approaches lean blowout. The intensity of these low-frequency fluctuations is used to detect the proximity to lean blowout and can be used as a control variable for active lean blowout suppression without knowing the lean-blowout fuel/air ratio limit. The tunable diode-laser sensor results are compared with traditional pressure and emission sensors, and the tunable diode-laser sensor is found to offer several advantages, including better spatial resolution and insensitivity to background acoustic noise and flame emissions.**

## Nomenclature

| | | |
|---|---|---|
| $a$ | = | wavelength-modulation depth |
| $D$ | = | quartz tube diameter |
| $d$ | = | swirler exit nozzle diameter |
| $E''$ | = | lower state energy |
| $H_2$ | = | second harmonic Fourier component |
| $h$ | = | height above the dump plane |
| $I$ | = | laser intensity |
| $L$ | = | path length |
| $P$ | = | pressure |
| $R_{2f}$ | = | wavelength-modulation spectroscopy $2f$ peak ratio |
| $r$ | = | radial distance from the centerline of the quartz tube |
| $S$ | = | line strength of absorption feature |
| $T$ | = | temperature |
| $t$ | = | time |
| $\varphi$ | = | line shape function |
| $\phi$ | = | equivalence ratio |
| $\phi_{\mathrm{LBO}}$ | = | lean blowout equivalence ratio |
| $\nu$ | = | laser output frequency |
| $\bar{\nu}$ | = | laser center frequency |
| $\tau$ | = | transmission coefficient |
| $\omega$ | = | wavelength-modulation angular frequency |

## I. Introduction

RECENT efforts to improve power and propulsion systems are mostly directed toward cleaner and more environmentally friendly power generation. Emissions legislation has motivated the development of combustors that operate at leaner fuel/air equivalence ratios, in which lower flame temperatures reduce the production of NOx [1,2]. In addition, these lean operating conditions reduce engine maintenance, because the lower combustion temperatures increase the lifetime of engine components [1]. However, fuel-lean combustion is susceptible to instabilities in the form of thermoacoustic oscillations and lean blowout (LBO), which pose a serious problem for the operation of low-emission gas turbine combustors.

Thermoacoustic instabilities refer to self-sustained combustion oscillations at or near the acoustic frequency of the combustion chamber, which are the result of the closed-loop coupling of unsteady heat release to pressure oscillations (Rayleigh criterion [3]). Unstable combustion may lead to decreased combustion efficiency, increased pollutant emissions, and system performance degradation [1]. Intensive experimental and theoretical work has been performed during the past decade to understand the driving mechanisms of thermoacoustic instabilities and to develop effective approaches to suppress these instabilities in laboratory-scale or full-scale combustors [4–9]. It is well known that heat release fluctuations produce pressure fluctuations; however, the mechanisms whereby pressure fluctuations result in heat release fluctuations are not well understood [4]. Equivalence ratio fluctuation [5,6] and flame-vortex interaction [4,9] are considered to be the most important of these mechanisms in fuel-lean gas turbine combustion systems. Because of the complex physical and chemical interactions involved in thermoacoustic instabilities, it is difficult to predict this unstable combustion behavior. Therefore, typically combustion instabilities have been reduced or eliminated in industrial combustors by passive or active control mechanisms [7–9]. Active control strategies using fuel modulation [8] and acoustic forcing [9] have been successfully demonstrated to decouple the pressure and heat release fluctuations.

Lean blowout usually occurs at lower equivalence ratios or during rapid transient processes and is also a major concern in modern, highly loaded land-based and aeroengine combustors. In a stationary gas turbine engine, such blowout events require a time-consuming system shutdown and restart procedure, which increases maintenance costs and reduces engine lifetime. Currently, LBO is

Presented as Paper 4395 at the 42nd AIAA/ASME/SAE/ASEE Joint Propulsion Conference, Sacramento, CA, 9–12 July 2006; received 3 May 2006; revision received 29 August 2006; accepted for publication 15 September 2006. Copyright © 2006 by the authors. Published by the American Institute of Aeronautics and Astronautics, Inc., with permission. Copies of this paper may be made for personal or internal use, on condition that the copier pay the $10.00 per-copy fee to the Copyright Clearance Center, Inc., 222 Rosewood Drive, Danvers, MA 01923; include the code $10.00 in correspondence with the CCC.

*Research Assistant, High Temperature Gasdynamics Laboratory, Department of Mechanical Engineering. Student Member AIAA.
†Research Assistant, High Temperature Gasdynamics Laboratory, Department of Mechanical Engineering. Student Member AIAA.
‡Senior Research Engineer, High Temperature Gasdynamics Laboratory, Department of Mechanical Engineering. Associate Fellow AIAA.
§Professor, High Temperature Gasdynamics Laboratory, Department of Mechanical Engineering. Fellow AIAA.

prevented by operating the combustor with a wide safety margin above the uncertain LBO equivalence ratio limit. This LBO limit varies with many operating parameters, including the air and fuel flow rates, fuel composition, and combustor age [10,11]. Consequently, NOx emission could be reduced and engine performance could be improved by operating with a narrower LBO safety margin.

A large amount of previous work has been performed to investigate the mechanisms of LBO as the equivalence ratio is reduced, with the general finding of a transition between stable flames and LBO that is characterized by an intermediate stage with large-scale unsteadiness and local extinction and reignition events [10–14]. Bradley et al. [12] showed that the flame is stabilized by hot gas in both the inner and outer recirculation zones at steady combustion, whereas the unstable flame near LBO is stabilized only by the hot gas in the inner zone. Several studies showed that if this large-scale unsteadiness is reduced, the LBO limit can be extended to lower equivalence ratios. Based on detection of LBO precursors using $OH^*$ chemiluminescence, Thiruchengode et al. [10] extended the LBO limit by modifying the fuel fraction injected into the flame stabilization zone. Gutmark et al. [15] extended the LBO limit of a premixed dump combustor by generating small-scale vortices using shear layer forcing, whereas Sturgess et al. [16] found that the LBO limit can be extended by exit blockage. Durbin and Ballal [17] observed that the LBO limit was reduced by increasing the outer swirl intensity if the inner swirl is stronger than the outer swirl.

Practical operation of low-emission gas turbine combustors will require real-time active control mechanisms to suppress thermoacoustic instabilities and avoid LBO. An important part of any control strategy is a robust sensor to measure a meaningful control variable. The most frequently used methods for instability sensing include acoustic detection using a microphone or pressure sensor and emission measurement from $OH^*$, $CH^*$, or $CO_2^*$ as a qualitative measure of the heat release rate [4–10]. However, these are volume sensors and, hence, their spatial resolution is generally quite different from the line-of-sight (LOS) diode-laser sensor. In addition, microphone sensors for pressure fluctuations are sensitive to background noise (from vibration or flow), and emission sensors may have interference from emissions of other radicals in the flame.

Gas temperature is a key parameter of the combustion process and, thus, has potential for use as a control variable in physics-based control strategies. Nonintrusive temperature measurements based on diode-laser absorption are particularly attractive and have been demonstrated in a variety of flowfields [18–21]. In previous work in our laboratory, a wavelength-multiplexed tunable diode-laser (TDL) sensor was used in a real-time adaptive control system to increase combustion efficiency and reduce emissions in a waste incinerator [22,23]. TDL temperature sensors offer potential for improved thermoacoustic instability and LBO control (relative to emission or acoustic sensors) owing to better spatial resolution and insensitivity to background noise and luminosity.

In this paper, a 2-kHz real-time (i.e., no postprocessing) temperature sensor using a single TDL near 1.4 $\mu$m is used to detect thermoacoustic instability and the proximity to LBO along an optimized LOS in a swirl-stabilized combustor, which serves as a model of gas turbine combustors. The TDL temperature sensor is based on absorption from two neighboring near-infrared (NIR) transitions of water vapor, an attractive target species because $H_2O$ is a major combustion product of hydrocarbon fuels. The selected line pair is free of interference from the absorption of other major combustion products. The temperature sensor also takes advantage of commercially available telecommunication fiber-coupled diode lasers and optics. Although gas composition and temperature are not completely uniform along the LOS, we show here that the TDL temperature sensor clearly identifies the high-frequency (hundreds of Hz) periodic oscillations and low-frequency ($\sim$10 Hz) fluctuations near LBO. The single-laser temperature sensor is first described and then used to monitor and suppress thermoacoustic instability through phase-delay feedback control. The TDL sensor is also used to characterize the flame behavior near LBO. The low-frequency temperature fluctuations are observed to increase sharply as the flame approaches LBO. Based on this signature, an active LBO control system can be developed for the swirl-stabilized combustor without knowing the actual LBO limit. In addition, the TDL sensor results are compared with traditional pressure and emission sensors.

## II. Theory

The development of the fast, single-laser temperature sensor for combustion gases has been described in detail previously [24]. In brief, a $H_2O$ line pair near 1.4 $\mu$m is targeted for nonintrusive measurements of gas temperature using a scanned-wavelength technique combined with wavelength-modulation spectroscopy (WMS) and $2f$ detection. Gas temperature is inferred from the ratio of WMS-$2f$ peak heights of the two selected $H_2O$ lines. The combination of scanned wavelength and wavelength modulation minimizes interference from flame emission and beam steering. By using WMS-$2f$ detection, the measurement sensitivity is improved by shifting the detection to higher frequencies at which laser excess noise and detector noise are both much smaller, and noise outside the detection bandwidth is suppressed by the phase-sensitive detection [24,25]. In addition, WMS-$2f$ detection using a lock-in amplifier simplifies data analysis and enables real-time measurements, resulting in a robust temperature sensor that is useful for combustion control applications. Real-time thermometry at 2 kHz has been demonstrated in gas- and liquid-fueled swirl-stabilized flames [25,26].

Here, we briefly present the related principles of the TDL WMS-$2f$ sensor. The transmission coefficient $\tau(\nu)$, of monochromatic radiation through a uniform medium, is given by the Beer–Lambert relation:

$$\tau(\nu) = (I_t/I_0)_\nu = \exp[-S\varphi_\nu P_i L] \tag{1}$$

where $I_t$ and $I_0$ are the transmitted and incident laser intensities, $S$ [$\mathrm{cm^{-2}/atm}$] and $\varphi_\nu$ [cm] are the line strength and line shape function for the absorption feature, $P_i$ [atm] is the partial pressure of the absorbing species, and $L$ [cm] is the path length.

For scanned WMS-$2f$ detection of the absorption, a fast wavelength scan is combined with a much faster sinusoidal wavelength modulation with angular frequency $\omega$, and the laser output frequency can be expressed by

$$\nu(t) = \bar{\nu}(t) + a\cos(\omega t) \tag{2}$$

where $\bar{\nu}(t)$ [$\mathrm{cm^{-1}}$] is the laser center frequency and $a$ [$\mathrm{cm^{-1}}$] is the modulation depth. The transmission coefficient $\tau(\nu) = \tau[\bar{\nu} + a\cos(\omega t)]$ is a periodic even function in $\omega t$ and can be expanded in a Fourier cosine series:

$$\tau[\bar{\nu} + a\cos(\omega t)] = \sum_{k=0}^{\infty} H_k(\bar{\nu}, a)\cos(k\omega t) \tag{3}$$

For optically thick samples, it is necessary to perform full simulations using Eqs. (1) and (3). However, the selected $H_2O$ transitions are optically thin ($S\varphi_\nu P_i L < 0.1$) for the experimental conditions encountered in this paper, and so the transmission coefficient reduces to

$$\tau(\nu) = \exp[-S\varphi_\nu P_i L] \approx 1 - S\varphi_\nu P_i L \tag{4}$$

and the second harmonic Fourier component is given by

$$H_2(\bar{\nu}, a) = -\frac{SP_iL}{\pi}\int_{-\pi}^{+\pi} \varphi(\bar{\nu} + a\cos\theta)\cos 2\theta \, \mathrm{d}\theta \tag{5}$$

The measured WMS-$2f$ signal is proportional to $I_0(\bar{\nu})H_2(\bar{\nu}, a)$ when laser intensity modulation and other nonlinear effects can be neglected for the small modulation depth used in this work [27,28]. Figure 1 illustrates the simulated WMS-$2f$ spectra for the selected $H_2O$ line pair of the TDL temperature sensor at four temperatures ($T$ = 300, 1000, 1500, and 2000 K; $P$ = 1 atm; 10% $H_2O$ in air; $L$ = 15 cm; and $a = 0.047\ \mathrm{cm^{-1}}$). The selected $H_2O$ line pair has large values of lower state energy: $E'' = 1789.0\ \mathrm{cm^{-1}}$ for the line at

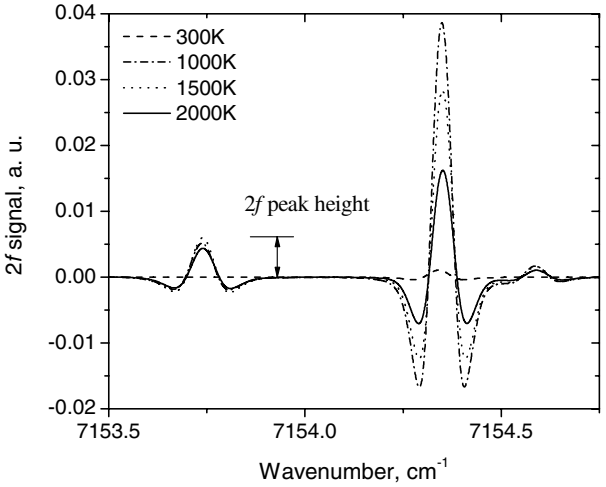


**Fig. 1 Simulated $H_2O$ WMS-2$f$ spectra at 300, 1000, 1500, and 2000 K for the TDL sensor; $P = 1$ atm, 10% $H_2O$ in air, $L = 15$ cm, and modulation depth $a = 0.047$ cm$^{-1}$.**

7154.35 cm$^{-1}$ and 2552.9 cm$^{-1}$ for the line at 7153.75 cm$^{-1}$, respectively. This line selection minimizes the interference from ambient water vapor and cold boundary layers and ensures that the temperature changes measured by the TDL sensor primarily reflect temperature fluctuations in the hottest regions of the burned gas [26]. Gas temperature can be obtained from the WMS-2$f$ peak height ratio of the two $H_2O$ transitions [24] and is closely related to the ratio of absorption line strengths, that is,

$$R_{2f} = \frac{I_0(\bar{\nu}_1)H_2(\bar{\nu}_1)}{I_0(\bar{\nu}_2)H_2(\bar{\nu}_2)} = \frac{I_0(\bar{\nu}_1)S_1(T)\int_{-\pi}^{+\pi}\varphi(\bar{\nu}_1 + a\cos\theta)\cos 2\theta\,\mathrm{d}\theta}{I_0(\bar{\nu}_2)S_2(T)\int_{-\pi}^{+\pi}\varphi(\bar{\nu}_2 + a\cos\theta)\cos 2\theta\,\mathrm{d}\theta} \tag{6}$$

As can be seen from the preceding equation, the WMS-2$f$ peak height ratio is not only a function of temperature through the line strength ratio, but also a function of gas composition through the effects of the line shape function. Figure 2 plots the simulated WMS-2$f$ peak ratio of the selected line pair as a function of temperature for various values of $H_2O$ mole fraction ($P = 1$ atm). A 20% change in $H_2O$ mole fraction produces a negligible change (1.8%) in the inferred gas temperature. Thus, for combustion gas conditions, a reliable determination of $R_{2f}$ yields an accurate determination of gas temperature.

It should be noted that use of the TDL sensor for precise temperature measurements may be complicated by the assumption of uniform gas composition and temperature along the LOS. For the

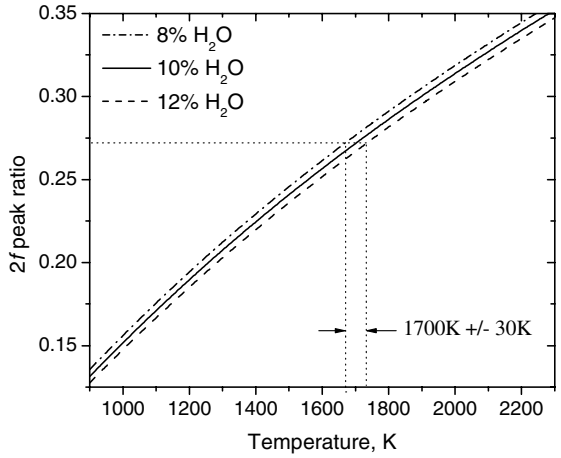


**Fig. 2 Simulated WMS-2$f$ peak ratio for the 7153.75 cm$^{-1}$/7154.35 cm$^{-1}$ line pair as a function of temperature for various values of $H_2O$ mole fraction; $P = 1$ atm and modulation depth $a = 0.047$ cm$^{-1}$.**

control applications presented in this paper, temperature changes and fluctuations of the flame are more important than the absolute values of temperature. The Fourier power spectrum of a time series of the detected WMS-2$f$ peak ratio $R_{2f}$ provides an excellent measure of temperature fluctuations in the hot burned gases. Furthermore, the WMS-2$f$ peak ratio is insensitive to any signal transmission losses common to the two closely spaced wavelengths of the water vapor transitions [26]. For example, the ratio is insensitive to scattering losses from liquid droplets or transmission losses from window fouling. Therefore, the WMS-2$f$ peak ratio is used in this work as a control variable for both thermoacoustic instability and LBO control experiments.

## III. Experiment Setup

### A. Swirl-Stabilized Combustor

The atmospheric pressure, swirl-stabilized dump combustor is propane-fueled with a thermal power of 20–60 kW and is shown schematically in Fig. 3. The combustor configuration was designed as a model of a lean, partially premixed turbine combustor that includes a triple annular research swirler (TARS); the details of this burner design are reported in [29]. The flow is from bottom to top. A combination of honeycomb and mesh screens are used to create a uniform air flow in the air-conditioning chamber. Four identical loudspeakers (75 W each) are mounted at the air-conditioning chamber for thermoacoustic instability control. The TARS has three air passages and the fuel injection points are uniformly distributed between the outer and intermediate swirlers (see the inset of Fig. 3). The diameter of the swirler exit nozzle is $d = 5.0$ cm. An outer (radial, counterclockwise 55 deg), intermediate (axial, 0 deg), and inner (axial, counterclockwise 45 deg) swirler configuration is used for the current work. The combustion chamber is bounded by a quartz tube ($D = 9.0$ cm diameter, 45-cm length for thermoacoustic instability experiments, and 20-cm length for LBO experiments), which permits uncooled operation of the combustor and provides optical access for the TDL sensor. The fuel flow and air flow rates are independently controlled by valves and measured using calibrated flow meters. The measurement uncertainty of the equivalence ratio is estimated to be 0.01.

### B. Measurement Techniques

Details of the TDL sensor were described previously [24,26] and are only briefly described here. A distributed feedback (DFB), fiber-coupled diode laser (NEL, NLK1E5E1AA) operating near 1.4 $\mu$m is driven by an external current modulation: a 2-kHz linear current ramp, yielding wavelength tuning over $\sim$2 cm$^{-1}$, summed with a 500-kHz sinusoidal current modulation generating $a = 0.047$ cm$^{-1}$. The laser beam is lens-collimated and directed across the flame at a height of 5 cm ($h/d = 1$) above the dump plane, which is defined as $h = 0$. The laser beam is intentionally aligned (2.5 cm, $r/d = 0.5$) off the centerline ($r = 0$) of the duct to maximize the sensitivity of the TDL sensor for instability sensing (see Secs. IV.A and V.A for details). A flat mirror provides a double-pass configuration to improve SNR (total path length $\sim$15 cm in the flame). The transmitted laser beam passes through a narrow bandpass filter (NB-1400-030-B, Spectrogon) and is monitored by an InGaAs detector (3-mm diameter active area, 4 MHz, Electro-optical Systems). The free space light paths external to the combustion chamber are purged by dry nitrogen to remove interference absorption by ambient water vapor in the room air. The detected signal is filtered with a 320-kHz high-pass filter and a 1.28-MHz low-pass filter (Frequency Devices, Inc.) to remove unwanted frequency components. The second harmonic component of the detector signal is measured with a Perkin–Elmer lock-in amplifier (model 7280) with a time constant of 1 $\mu$s. Two-kHz real-time data processing, including peak finding and ratio calculation, is achieved by a fast PC combined with a laboratory code written in C++ [24].

Acoustic signals from the flame are measured by a Brüel & Kjær microphone (model 4939-A-011) located 0.3 m away from the combustion chamber. CH* chemiluminescence is also detected to

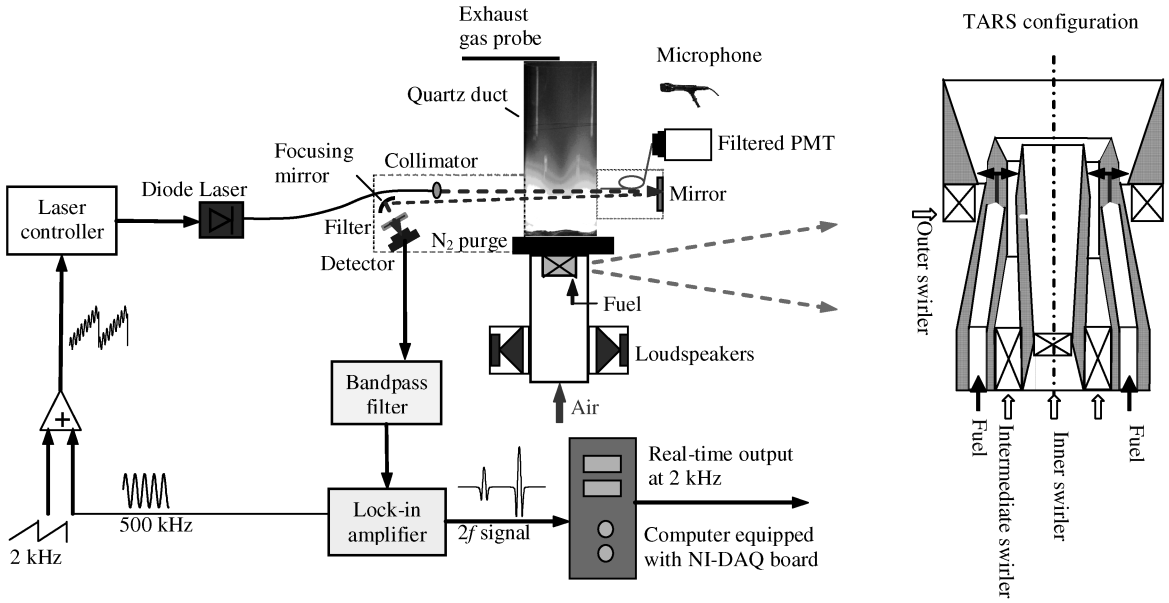


**Fig. 3 Schematic diagram of the real-time TDL temperature sensor and the swirl-stabilized combustor; burner described in detail in [29].**

qualitatively monitor the time-varying heat release. The light emitted by the flame is collected by a fused silicon fiber (placed ~5 cm above the dump plane, shown in Fig. 3) in a cone angle of about 23 deg. The light is filtered by a 10-nm bandpass filter centered at 430 nm and detected with a photomultiplier tube (PMT, Hamamatsu R928).

The CO and NOx concentrations in the exhaust gas are measured by gas sampling (choked flow) with a water-cooled quartz probe at the center of the exhaust plane of the combustion chamber. The samples are drawn through a cooled water trap (maintained at 3°C) and a drying column to reduce the water mole fraction. The dry CO and NOx concentrations are measured with commercial analyzers: MLT NGA2000 analyzer (Rosemount Analytical) and a chemiluminescence NOx analyzer (Teledyne Instruments, model 200E), respectively. Both gas analyzers are zeroed by $N_2$ and calibrated by span gases before the combustion measurements.

## IV. Monitoring and Suppressing Thermoacoustic Instability

### A. Monitoring Thermoacoustic Instability

In the swirl-stabilized combustor, the flame is stabilized by the recirculation zones in the flowfield: a central recirculation zone (CRZ) created by the swirl and an outer recirculation zone (ORZ) created by the sudden expansion [12]. Figure 4 illustrates the schematic of the flowfield and flame structure in our combustor. The recirculation zones produce a region of low velocity with long residence time that allows the flame to propagate into incoming fresh mixture and, thus, serve as a source of continuous ignition for the combustible fuel/air mixture [30]. In stable combustion, most of the chemical reaction occurs between the two hot recirculation zones (see the flame picture in Fig. 3), and the flame tip is about 5 cm ($h/d = 1$) above the dump surface.

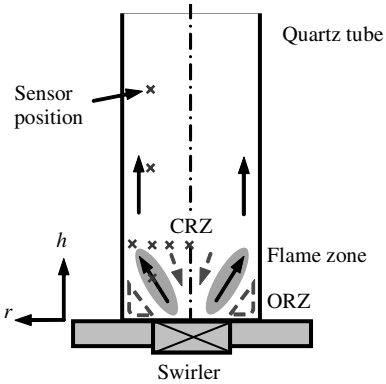


**Fig. 4 Schematic of the stable flame structure with central and outer recirculation zones in the flowfield. Also indicated are the investigated TDL sensor locations in the flame.**

Because the TDL sensor is a LOS measurement, it is important to optimize the positioning of the laser beam. To investigate the effect of laser positioning, a 100-Hz oscillation was introduced in the flame by modulating the intake air flow with four loudspeakers attached to the air-conditioning chamber (Fig. 3). To optimize the sensor LOS, measurements were conducted at different horizontal and vertical locations in the forced flame with an air flow rate of 400 SLM (standard liters per minute) and propane flow rate of 9.9 SLM ($\phi = 0.58$).

The measured FFT power spectra of the TDL sensor at four horizontal locations ($h = d = 5$ cm) are shown in Fig. 5. At positions very near the wall ($r/d > 0.75$), TDL sensor measurements are contaminated by additional low-frequency temperature fluctuations in the boundary layer. At positions near the centerline ($r/d = 0.02$), the TDL sensor poorly identifies the temperature oscillation at 100 Hz, because different regions along the sensor LOS oscillate at different phases and the strength of the oscillation is reduced in the path-integrated TDL measurement. We find excellent identification of the flame oscillation in the region $0.2 < r/d < 0.7$ and, hence, we selected the location $r/d = 0.5$ as the best position for the TDL sensor LOS to monitor temperature oscillations.

Similarly, we investigated the best vertical position for the TDL sensor LOS. Figure 6 plots the measured FFT power spectra of the TDL sensor at four vertical locations ($r = 2.5$ cm). For sensor positions high in the flame ($h/d > 2$), the signature of the oscillation is nearly buried in the noise because of the mixing of gases from the different regions of the combustor. For $h/d < 0.5$, no flame is observed along the sensor LOS due to the flame structure. For the range $0.5 < h/d < 1.5$, the TDL sensor clearly identifies the flame oscillation. These experiments show that the best region for sensing temperature oscillations is near the flame tip ($h/d \sim 1$ and $r/d \sim 0.5$); however, good performance (signal-to-noise ratio larger than 10) is observed over a wide range of positions ($0.5 < h/d < 1.5$ and $0.2 < r/d < 0.7$) and the sensor LOS does not need to be precisely located.

The TDL sensor is also used to monitor the natural thermoacoustic instability induced by the round quartz duct. Figure 7a shows the measured temperature and its FFT power spectrum for a laser LOS near the flame tip with an air flow rate of 820 SLM and propane flow rate of 39.6 SLM ($\phi = 1.1$). A time resolution of 0.5 ms is achieved with a laser scan rate of 2 kHz, and an FFT is performed on 0.5 s of

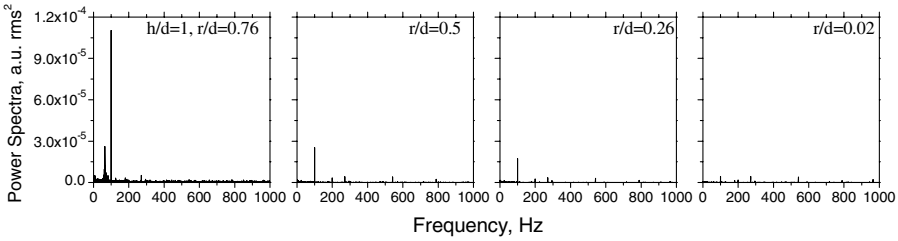


**Fig. 5 Measured FFT power spectra of TDL sensor at four horizontal locations in the forced flame; $h/d = 1$.**

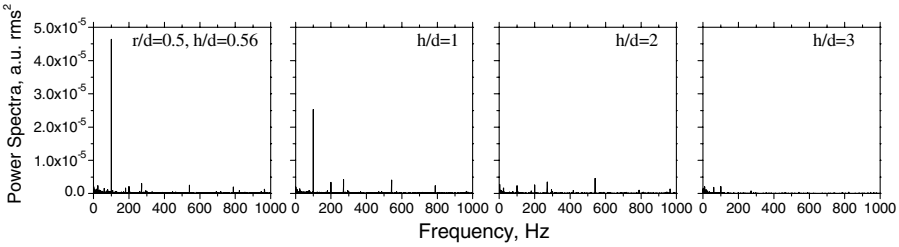


**Fig. 6 Measured FFT power spectra of TDL sensor at four vertical locations in the forced flame; $r/d = 0.5$.**

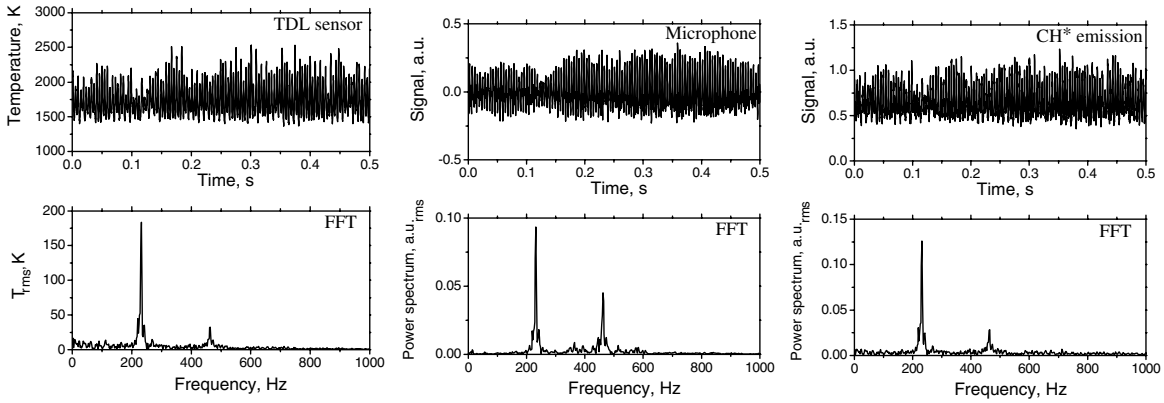


**Fig. 7 Measured signals and FFT power spectra of: a) TDL sensor, b) microphone, and c) CH* chemiluminescence; propane/air flame.**

temperature data, providing a resolution of 2 Hz. The measured acoustic signal and CH* chemiluminescence are also shown in Fig. 7 for comparison. The dominant oscillation mode (232 Hz) and its harmonic (464 Hz) can be clearly seen from the FFT spectra of three sensors. This confirms the interpretation of the temperature data: thermoacoustic instability is the coupling of unsteady heat release to acoustic oscillations. The measurements illustrate qualitative comparison of the three sensors, although the positions of the chemiluminescence and acoustic detectors were not optimized and the signal strengths were not calibrated. The TDL sensor has some potential advantages for instability control, owing to its spatial resolution and insensitivity to background noise and luminosity.

### B. Active Control of Thermoacoustic Instability

The TDL sensor can accurately identify flame oscillations and can be used in an active control system to suppress these instabilities. A phase-delay feedback control strategy was used for the demonstration described here. Figure 8 illustrates the experiment setup. The 2 kHz real-time sensor output is first time-delayed (dSPACE 1104 board), and this delayed signal is filtered (SR640 low-pass filter and SR645 high-pass filter) and amplified (Phast Landmark, PLB-AMP8) to drive the loudspeakers to modulate the intake air flow. The gain of the feedback system is related to the transfer function of the loudspeaker actuation on the air flow. The absolute gain is not quantified, as only the relative gain of the amplifier is used to optimize the control.

Experiments were carried out with a propane flow rate of 31.1 SLM and air flow rate of 796 SLM ($\phi = 0.93$). Figure 9 plots the power spectra of the TDL sensor output. Without control, a 388-Hz oscillation is clearly seen in the spectrum [Fig. 9a], whereas with control, the thermoacoustic instability is successfully suppressed by the phase-delay feedback control with a time delay of 2 ms and a relative gain of 50. Note the duct used for this experiment is slightly

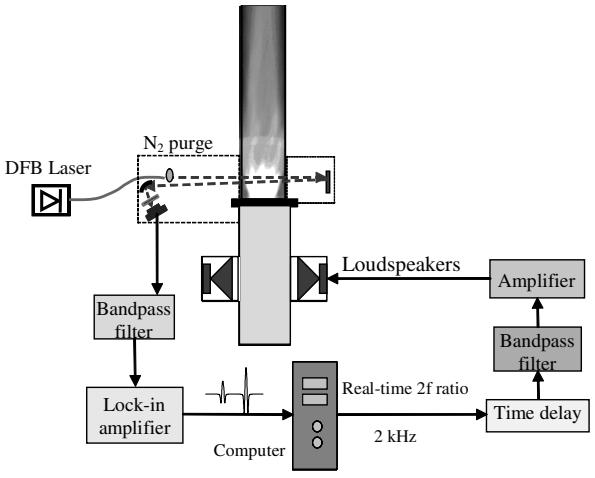


**Fig. 8 Experiment setup for phase-delay feedback control of thermoacoustic instability.**

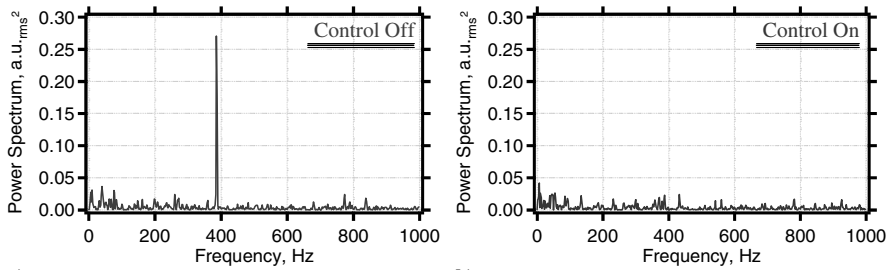


**Fig. 9 FFT power spectra of the real-time temperature sensor output: a) control off and b) control on.**

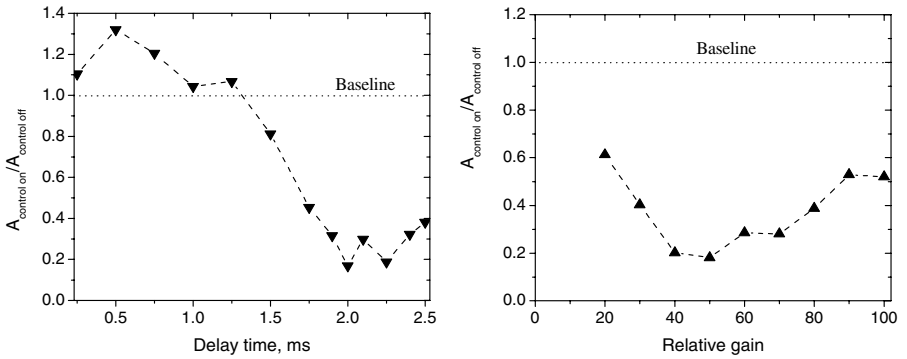


**Fig. 10 Amplitude of the temperature oscillations at the instability frequency for a) various delay times and b) various relative gains in the phase-delay feedback control system.**

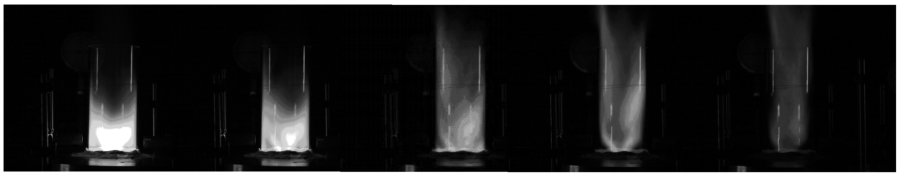


**Fig. 11 Flame structure from stable combustion to near LBO ($\phi_{LBO} = 0.44$).**

different from that used in Fig. 7, hence, the oscillation frequencies are different.

According to the Rayleigh criterion, the coupling between the pressure oscillation and the unsteady heat release must be interrupted to suppress combustion oscillations. Experiments were also performed to investigate the effects of phase delay and relative gain on the active control results. The variation of the temperature oscillations as a function of the delay time of the phase-delay board is shown in Fig. 10a for the instability at 388 Hz (relative gain is 50). Note that the absolute value of the delay time is arbitrary, as it includes delay in the control electronics and flow time. The controlled behavior is compared with the straight horizontal line that depicts the temperature oscillations when the controller is not operating. Maximum suppression is obtained at a time delay of 2 ms, whereas maximum destabilization of the combustion is observed at 0.5 ms, which is approximately at 200 deg from the optimal phase. At the optimal delay-time, the instability is suppressed by more than 7 dB. The variation of the temperature oscillations as a function of relative gain is also shown in Fig. 10b (delay time is 2 ms), and maximum suppression is obtained at a relative gain of 50. These results clearly indicate that the TDL sensor can accurately identify the frequency, phase, and amplitude of the flame instability and provide the appropriate feedback for the active control system. More advanced control strategies (e.g., adaptive control) and other actuation methods (e.g., secondary fuel injection) are, of course, possible with this sensor for active control of practical large-scale combustors.

## V. Sensing for LBO Control

### A. Characterizing the LBO Process

Figure 11 shows the pictures of flame as the fuel is reduced from stable combustion to near LBO for a constant air flow rate. A stable flame is anchored to both the CRZ and ORZ. However, the quenching by flame stretch becomes more important near LBO. There is less heat release between two recirculation zones and more reaction occurs downstream along the wall, resulting in less intense combustion; hence, the flame loses its anchor with the ORZ and becomes unstable. These observations are consistent with the recirculation zone stabilization mechanism of a swirl-stabilized combustor reported by [12]. These flame structures suggest the best location for the sensor LOS for LBO sensing is the shear layer between the CRZ and ORZ or wall (see Fig. 4).

The TDL temperature sensor was used to characterize the flame behavior as the equivalence ratio was reduced; the first results were presented in [26]. In these experiments, the fuel flow rate was decreased gradually, while holding the air flow constant, until LBO occurs. The power spectrum is calculated by a FFT algorithm for every 0.5-s series of recorded WMS-2$f$ peak ratio. Figure 12 plots the FFT power spectra of the TDL sensor at two different equivalence ratios: $\phi$-$\phi_{LBO} = 0.40$ and 0.02 (sensor location: $h/d = 1$, $r/d = 0.5$). The noise in Fig. 12a is nearly white and typical for steady combustion conditions, whereas the low-frequency fluctuations in Fig. 12b are typical for near-blowout conditions. The data in Fig. 12b illustrate that these low-frequency components

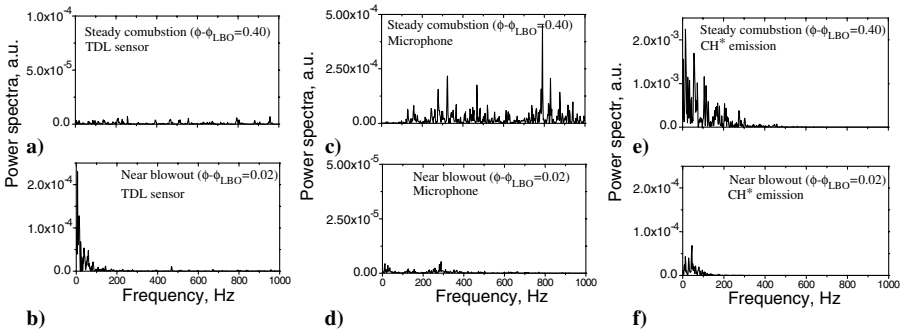


**Fig. 12 FFT power spectra of the TDL sensor, microphone, and CH* emission at two different conditions; TDL sensor location is $h/d = 1$ and $r/d = 0.5$.**

increase significantly as the flame approaches LBO, which is consistent with the increase of local extinction/reignition events. There is no characteristic frequency in the power spectrum, because the flame extinction events occur randomly. FFT power spectra of the microphone signal and CH* emission at steady combustion and near-LBO conditions are also shown in Fig. 12 for comparison. The absolute magnitude of the acoustic and CH* emission signals have large variation from the noisy, bright steady combustion to the quiet, dark flame near LBO. These data illustrate the large dynamic range required for LBO detection with the microphone or emission sensors, whereas the transmitted laser intensity remains strong for flames near LBO. Thus, an advantage of the TDL sensing over the traditional sensors for LBO detection is the large signal on a quiet background for the low-frequency temperature fluctuations.

The fraction of FFT power in the 0–50 Hz range, $\mathrm{FFT\%_{[0–50\ Hz]}}$, is used to characterize the low-frequency temperature fluctuations [26]. To investigate the effect of laser beam positioning, measurements were conducted at different horizontal and vertical locations in the propane/air flame. Figure 13 shows the measured $\mathrm{FFT\%_{[0–50\ Hz]}}$ as a function of the equivalence ratio at four different horizontal locations (airflow rate is 728 SLM). It is clear that location $r/d = 0.5$ (across the flame) is the best position for the TDL sensor LOS to detect low-frequency temperature fluctuations, which increase sharply as the flame approaches LBO. Approximately 10% of power is in the 0–50 Hz range when combustion is steady, but increases up to 90% near LBO. At positions very near wall ($r/d > 0.75$), no flame is observed along the sensor LOS near LBO, because the flame is located downstream of the sensor. At positions near the centerline ($r/d = 0.02$), we find additional low-frequency temperature fluctuations even for equivalence ratios with stable flames due to the fully reacted gases in the CRZ.

Similar experiments were carried out for different vertical locations ($r/d = 0.5$), as shown in Fig. 14. The best vertical location for the TDL sensor is at the tip of the flame during stable combustion ($h/d = 1$). At positions well above the flame tip ($h/d > 3$), additional low-frequency temperature fluctuations are observed even for stable flames due to the effect of gas mixing. At positions very low in the flame ($h/d < 0.5$), occasionally no flame is observed along the sensor LOS due to the asymmetric flame structure near LBO. Therefore, the most effective location for the TDL sensor for LBO sensing is at the tip of the flame during stable combustion, that is, $h/d \sim 1$ and $r/d \sim 0.5$ for current combustor configuration, which is similar to the optimum position found for thermoacoustic instability detection. Good LBO sensing (contrast between near LBO and steady combustion larger than five) is observed over a wide range of positions ($0.5 < h/d < 2$ and $0.25 < r/d < 0.6$) and the sensor does not need to be precisely located.

Similar behavior was observed at various air flow rates from 440 to 980 SLM. For a specific air flow, the LBO stoichiometry is observed to be repeatable within 0.01, and the LBO limit increases with air flow rate (from 0.33 to 0.49 for the tested air flows), as illustrated in Fig. 15.

### B. Detecting Proximity to LBO

The measured increase in low-frequency temperature fluctuations can be used to detect the proximity to LBO without knowing the actual LBO limit for a specific operating condition. Figure 16a plots the measured $\mathrm{FFT\%_{[0–50\ Hz]}}$ as a function of the equivalence ratio and

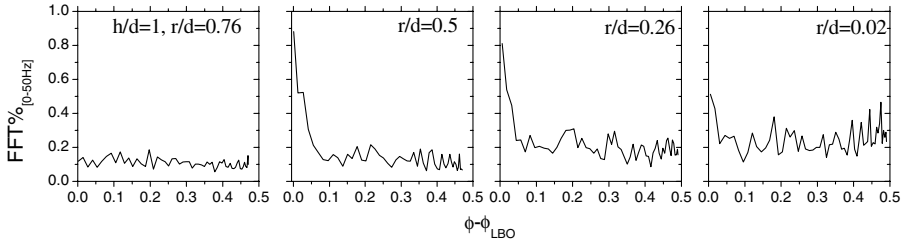


**Fig. 13 Fraction of FFT power in 0–50 Hz of the TDL sensor as a function of the equivalence ratio at four horizontal locations; $h/d = 1$ and air flow rate is 728 SLM.**

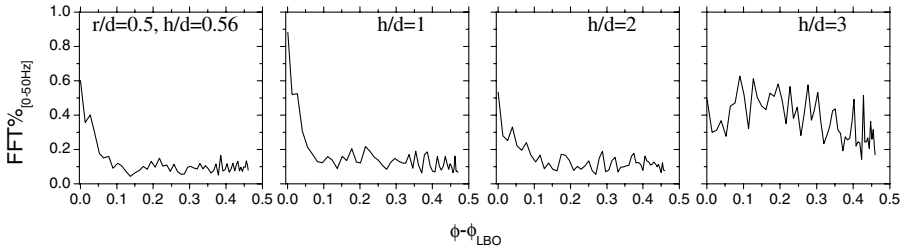


**Fig. 14 Fraction of FFT power in 0–50 Hz of the TDL sensor as a function of the equivalence ratio at four vertical locations; $r/d = 0.5$ and air flow rate is 728 SLM.**

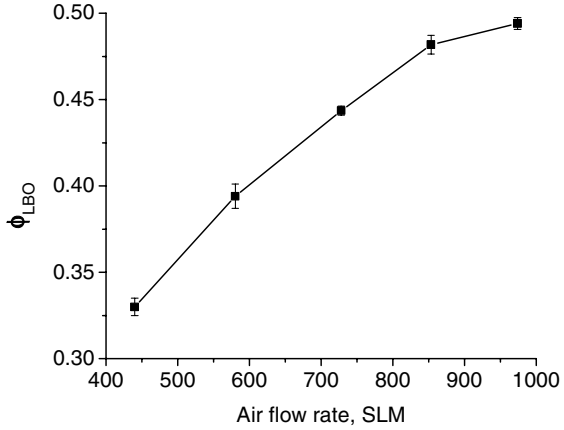


**Fig. 15 LBO equivalence ratio as a function of air flow rate.**

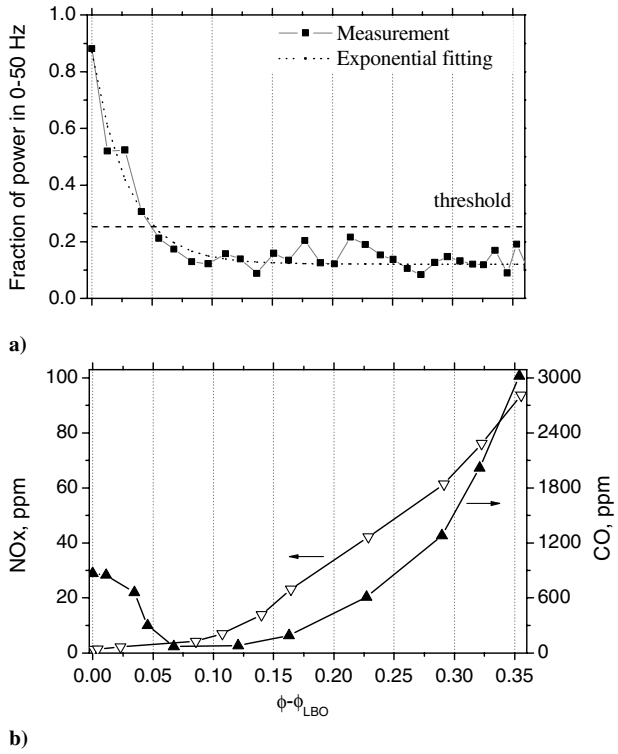


**Fig. 16 Detecting the proximity to LBO: a) fraction of FFT power in 0–50 Hz of the TDL sensor output and b) measured CO and NOx concentrations (dry-based) in the exhaust gas as a function of the equivalence ratio; air flow rate is 728 SLM.**

the best fit to the exponential control model [26]:

$$\text{FFT}\,\%_{[0\text{–}50\ \text{Hz}]} = \frac{T_{\text{rms}^2[0,50]}}{T_{\text{rms}^2[0,1000]}} = 0.75\exp[-(\phi - \phi_{\text{LBO}})/0.03] + 0.12 \tag{7}$$

A threshold value for $\text{FFT}\%_{[0\text{–}50\ \text{Hz}]}$ that is larger than all values of $T_{\text{rms}^2[0,50]}/T_{\text{rms}^2[0,1000]}$ for steady combustion can be set to distinguish near-blowout conditions from steady conditions [26]. As shown by the flame structure in Fig. 11, there is an unstable flame range between stable combustion and LBO. This unstable flame range ($\phi$-$\phi_{\text{LBO}} < 0.05$) is successfully identified by the TDL sensor (Fig. 16a) and exists for all conditions studied. For this combustor, we found that the same threshold ($\text{FFT}\%_{[0\text{–}50\ \text{Hz}]} = 0.25$) is suitable to detect LBO for all air flow rates.

The CO and NOx concentrations measured in the exhaust gas are consistent with the LBO sensing with the TDL sensor, as shown in Fig. 16b. The NOx concentration decreases as the equivalence ratio is reduced, mainly due to lower combustion temperature, and a minimum NOx concentration as low as 1 ppm is observed near LBO. The CO concentration decreases as the equivalence ratio is reduced when the flame is stable, but increases near $\phi$-$\phi_{\text{LBO}} = 0.05$ as the low-frequency fluctuations begin, in good agreement with the measurements in a similar combustor [29]. Local extinction and reignition events near LBO lead to reduced combustion efficiency and increased CO concentration. Therefore, for the current combustor, the optimum operating condition for ultralean, low-emission combustion is $\phi$-$\phi_{\text{LBO}} \sim 0.05$. Because the LBO limit depends on flow rates as well as other operating parameters, an active control system is required to achieve this optimum operation. The TDL sensor can be used to detect the proximity to LBO and provide a control variable ($\text{FFT}\%_{[0\text{–}50\ \text{Hz}]}$) for the active suppression of LBO. Active feedback control has been demonstrated in our combustor to prevent LBO with a very narrow LBO margin and, thus, reduced pollutant emissions [26].

## VI. Conclusions

A tunable diode-laser temperature sensor has been applied to monitor and control thermoacoustic instability and LBO in propane/air flames in an atmospheric pressure, swirl-stabilized combustor that serves as a model of gas turbine combustors. The real-time (2 kHz) temperature sensor is based on TDL absorption of $H_2O$ in the NIR and uses only one telecom fiber-coupled DFB diode laser. Detailed experiments were conducted to optimize the position of the sensor LOS in the flame for thermoacoustic instability and LBO sensing. The TDL sensor accurately identified the frequency, phase, and amplitude of the flame oscillation and was used in the phase-delay feedback control system to suppress the thermoacoustic instability. An acoustic actuation was employed to modulate the air flow before it entered the swirl-stabilized combustor, thus interrupting the coupling of unsteady heat release to pressure oscillations. At the optimal control conditions, the temperature oscillations were suppressed by more than 7 dB.

The TDL sensor was also used to characterize the LBO process. It was found that low-frequency temperature fluctuations increase near LBO, with the fraction of FFT power in the 0–50 Hz range increasing sharply. These low-frequency temperature fluctuations were used to sense the proximity to LBO and can be used as a control variable for an active LBO control system without knowing the actual LBO limit.

The TDL sensor can offer some advantages over traditional pressure and emission sensors for instability and LBO sensing. These advantages can arise because of the TDL sensor's localized LOS. In addition, the TDL sensor is insensitive to background acoustic noise and flame emissions. Traditional sensors have diminished signals when the flame approaches LBO, whereas the TDL signal remains strong.

## Acknowledgments

We gratefully acknowledge support from the Office of Naval Research (via the University of Cincinnati), the Air Force Office of Scientific Research, and the Global Climate and Energy Project at Stanford University. We thank Ephraim Gutmark for sharing his design of the swirl-stabilized combustor.

## References

[1] Lefebvre, A. H., *Gas Turbine Combustion*, Edwards Brothers, Ann Arbor, MI, 1999.

[2] Martin, R. J., and Brown, N. J., "Nitrous Oxide Formation and Destruction in Lean, Premixed Combustion," *Combustion and Flame*, Vol. 80, Nos. 3–4, 1990, pp. 238–255.

[3] Rayleigh, J. W. S., *The Theory of Sound 2*, Dover, New York, 1945.

[4] Lee, J. G., and Santavicca, D. A., "Experimental Diagnostics for the Study of Combustion Instabilities in Lean Premixed Combustors," *Journal of Propulsion and Power*, Vol. 19, No. 5, 2003, pp. 735–750.

[5] Liuwen, T., Torres, H., Johnson, C., and Zinn, B. T., "A Mechanism of Combustion Instability in Lean Premixed Gas Turbine Combustors," *Journal of Engineering for Gas Turbines and Power*, Vol. 123, No. 1,

2001, pp. 182–189.
[6] Duan, X. R., Meier, W., Weigand, P., and Lehmann, B., "Phase-Resolved Laser Raman Scattering and Laser Doppler Velocimetry Applied to Periodic Instabilities in a Gas Turbine Model Combustor," *Applied Physics B (Lasers and Optics)*, Vol. 80, No. 3, 2005, pp. 389–396.
[7] Dowling, A. P., and Morgans, A. S., "Feedback Control of Combustion Oscillations," *Annual Review of Fluid Mechanics*, Vol. 37, 2005, pp. 151–182.
[8] Neumeirer, Y., and Zinn, B. T., "Experimental Demonstration of Active Control of Combustion Instabilities Using Real-Time Modes Observation and Secondary Fuel Injection," *Twenty-Sixth Symposium (International) on Combustion*, Combustion Inst., Pittsburgh, PA, 1996, pp. 2811–2818.
[9] Paschereit, C. O., Gutmark, E., and Weisenstein, W., "Control of Thermoacoustic Instabilities and Emissions in an Industrial-Type Gas-Turbine Combustion," *Twenty-Seventh Symposium (International) on Combustion*, Combustion Inst., Pittsburgh, PA, 1998, pp. 1817–1824.
[10] Thiruchengode, M., Nair, S., Prakash, S., Scarborough, D., Neumeier, Y., Lieuwen, T., Jagoda, J., Seitzman, J., and Zinn, B., "An Active Control System for LBO Margin Reduction in Turbine Engines," 41st AIAA Aerospace Sciences Meeting and Exhibit, AIAA Paper 2003-1008, Reno, NV, 2003.
[11] Ateshkadi, A., McDonell, V. G., and Samuelsen, G. S., "Lean Blowout Model for a Spray-Fired Swirl-Stabilized Combustor," *Proceedings of the Combustion Institute*, Vol. 28, No. 4, Combustion Inst., Pittsburgh, PA, 2000, pp. 1281–1288.
[12] Bradley, D., Gaskell, P. H., Gu, X. J., Lawes, M., and Scott, M. J., "Premixed Turbulent Flame Instability and NO Formation in a Lean-Burn Swirl Burner," *Combustion and Flame*, Vol. 115, 1998, pp. 515–538.
[13] Chao, Y. C., Chang, Y. L., Wu, C. Y., and Cheng, T. S., "An Experimental Investigation of the Blowout Process of a Jet Flame," *Proceedings of the Combustion Institute*, Vol. 28, Combustion Inst., Pittsburgh, PA, 2000, pp. 335–342.
[14] Nair, S., Rajaram, R., Meyers, A. J., and Lieuwen, T. C., "Acoustic and Ion Sensing of Lean Blowout in an Aircraft Combustor Simulator," 43rd AIAA Aerospace Sciences Meeting and Exhibit, AIAA Paper 2005-932, Reno, NV, 2005.
[15] Gutmark, E. J., Parr, T. P., Wilson, K. J., Hanson-Parr, D. M., and Schadow, K. C., "Closed-Loop Control in a Flame and a Dump Combustor," *IEEE Control Systems Magazine*, Vol. 13, No. 2, 1993, pp. 74–78.
[16] Sturgess, G. J., Heneghan, S. P., Vangsness, M. D., Ballal, D. R., Lesmerises, A. L., and Shouse, D., "Effects of Back-Pressure in a Lean Blowout Research Combustor," *Journal of Engineering for Gas Turbines and Power*, Vol. 115, No. 3, 1993, pp. 486–498.
[17] Durbin, M. D., and Ballal, D. R., "Studies of Lean Blowout in a Step Swirl Combustor," *Journal of Engineering for Gas Turbines and Power*, Vol. 118, No. 1, 1996, pp. 72–77.
[18] Philippe, L. C., and Hanson, R. K., "Laser Diode Wavelength Modulation Spectroscopy for Simultaneous Measurement of Temperature, Pressure, and Velocity in Shock-Heated Oxygen Flows," *Applied Optics*, Vol. 32, No. 30, 1993, pp. 6090–6103.
[19] Allen, M. G., "Diode Laser Absorption Sensors for Gas-Dynamics and Combustion Flows," *Measurement Science and Technology*, Vol. 9, No. 4, 1998, pp. 545–562.
[20] Sanders, S. T., Baldwin, J. A., Jenkins, T. P., Baer, D. S., and Hanson, R. K., "Diode-Laser Sensor for Monitoring Multiple Combustion Parameters in Pulse Detonation Engines," *Proceedings of the Combustion Institute*, Vol. 28, Combustion Inst., Pittsburgh, PA, 2000, pp. 587–594.
[21] Teichert, H., Fernholtz, T., and Ebert, V., "Simultaneous in situ Measurement of CO, $H_2O$, and Gas Temperature in a Full-Sized Coal-Fired Power Plant by Near-Infrared Diode Lasers," *Applied Optics*, Vol. 42, No. 12, 2003, pp. 2043–2051.
[22] Furlong, E. R., Baer, D. S., and Hanson, R. K., "Combustion Control Using a Multiplexed Diode-Laser Sensor System," *Twenty-Sixth Symposium (International) on Combustion*, Combustion Inst., Pittsburgh, PA, 1996, pp. 2851–2858.
[23] Furlong, E. R., Baer, D. S., and Hanson, R. K., "Real-Time Adaptive Combustion Control Using Diode-Laser Absorption Sensors," *Twenty-Seventh Symposium (International) on Combustion*, Combustion Inst., Pittsburgh, PA, 1998, pp. 103–111.
[24] Zhou, X., Jeffries, J. B., and Hanson, R. K., "Development of a Fast Temperature Sensor for Combustion Gases Using a Single Tunable Diode Laser," *Applied Physics B (Lasers and Optics)*, Vol. 81, No. 5, 2005, pp. 711–722.
[25] Zhou, X., Jeffries, J. B., Hanson, R. K., Li, G., and Gutmark, E. J., "Fast Temperature Sensor for Combustion Control Using H2O Diode Laser Absorption Near 1.4 $\mu$m," 43rd AIAA Aerospace Science Meeting and Exhibit, AIAA Paper 2005-627, Reno, NV, 2005.
[26] Li, H., Zhou, X., Jeffries, J. B., and Hanson, R. K., "Active Control of Lean Blowout in a Swirl-Stabilized Combustor Using a Tunable Diode Laser," *Proceedings of the Combustion Institute* (to be published).
[27] Liu, J. T. C., Jeffries, J. B., and Hanson, R. K., "Wavelength Modulation Absorption Spectroscopy with 2$f$ Detection Using Multiplexed Diode Lasers for Rapid Temperature Measurements in Gaseous Flows," *Applied Physics B (Lasers and Optics)*, Vol. 78, Nos. 3–4, 2004, pp. 503–511.
[28] Li, H., Rieker, G. B., Liu, X., Jeffries, J. B., and Hanson, R. K., "Extension of Wavelength-Modulation Spectroscopy to Large Modulation Depth for Diode Laser Absorption Measurements in High-Pressure Gases," *Applied Optics*, Vol. 45, No. 5, 2006, pp. 1052–1061.
[29] Li, G., and Gutmark, E. J., "Experimental Study of Flow Patterns and Reaction in a Multiple Swirl Spray Combustor," 41st AIAA Aerospace Sciences Meeting and Exhibit, AIAA Paper 2003-489, Reno, NV, 2003.
[30] Sturgess, G. J., Sloan, D. G., Lesmerises, A. L., Heneghan, S. P., and Ballal, D. R., "Design and Development of a Research Combustor for Lean Blow-Out Studies," *Journal of Engineering for Gas Turbines and Power*, Vol. 114, No. 1, 1992, pp. 13–19.

R. Lucht
*Associate Editor*